ANALYSIS OF THE PHYSICO-CHEMICAL MECHANISMS RESPONSIBLE FOR HYDROGEN ATTACK

S. M. Schlögl and E. Van der Giessen

Koiter Institute Delft, Delft University of Technology, The Netherlands

ABSTRACT

The failure mode known as 'hydrogen attack' involves several processes which are active when steel components are exposed to high hydrogen pressures at elevated temperatures. In this paper, a microstructural model is presented which covers these processes through a combination of continuum mechanics with solid solution thermodynamics, kinetics and chemistry. The model is applied to study the response of 2.25Cr-1Mo steel consisting of a ferritic matrix and alloy carbides (e.g., M_7C_3, $M_{23}C_6$, M_6C, M_2C) to an exposure of 18MPa hydrogen pressure at a temperature of 530°C. The investigated microstructures vary in their carbide types and/or their carbide volume fractions. The numerical simulations show that the microstructure that does not contain M_7C_3 carbides is most resistant to hydrogen attack.

KEYWORDS

hydrogen attack, 2.25Cr-1Mo steel, diffusion, dissolution, methane pressure, creep, driving force

INTRODUCTION

2.25Cr-1Mo steel is a standard material for reactors used in the petro-chemical industries. In case of hydrocracking or hydrotreating applications, the material of the reactor is exposed to a high hydrogen pressure and to elevated temperatures. It is this combination that is responsible for the material degradation process called hydrogen attack (HA). During HA, carbon, present in the steel, and hydrogen, originating from the gas atmosphere inside the reactor, form methane molecules. These molecules are captured in cavities which have nucleated at the grain boundaries. Due to the presence of methane and hydrogen molecules, the cavities are internally pressurized. Consequently, the cavities grow and coalesce which finally results in intergranular fracture.

Carbon is present in the steel in two forms, namely interstitially dissolved in the ferritic matrix (α-Fe) and bonded in carbides. A standard 2.25Cr-1Mo steel contains various types of carbides, such as M_7C_3, $M_{23}C_6$, M_6C and M_2C [1]. The microstructure, characterized by the composition of the various alloy carbides and their volume fraction, depends on the heat treatment. Generally, the steel that is exposed to the high hydrogen pressure, does not possess a microstructure which is in equilibrium. So, the question arises whether this influences the susceptibility to hydrogen attack. Our recently developed microstructural model [2] enables us to shed some light on this issue. In this paper, we numerically study the response of non-equilibrium microstructures and compare their resulting methane pressures and void growth to the ones of the equilibrium microstructure.

MICROSTRUCTURAL MODEL

The microstructure is represented by a spherical unit cell of radius r_o, in which a total of N carbides with the radius ρ^j are embedded. The unit cell is also assumed to contain one already nucleated cavity of radius a. Inside this cavity, the hydrogen pressure is taken to be the same as the one in the gas atmosphere inside the reactor or autoclave. Our microstructural model includes several mechanisms that are potentially relevant during hydrogen attack. These processes can be gathered in three groups (see Figure 1): (i) carbide dissolution controlled by the diffusion of metal and carbon atoms in the ferritic matrix away from or to the carbides (Figure 1a); (ii) chemical reaction of carbon and hydrogen in the void going hand in hand with the diffusion of carbon atoms to the void (Figure 1b) and (iii) growth of the void by grain boundary diffusion and dislocation creep (Figure 1c). Each of these groups is treated in a submodel. In this paper we briefly summarize the main ideas of the concept; for a complete description we refer to [2].

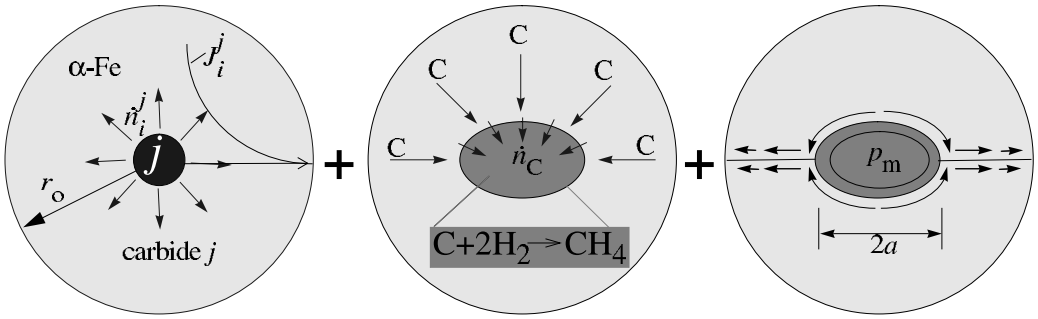

Figure 1: Submodels describing the processes leading to hydrogen attack. Submodel 1: dissolution of carbide j with radius ρ^j in the ferritic matrix together with the flux J_i^j leading to a homogeneous distribution in the ferrite (a). Submodel 2: chemical reaction of $\dot{n}_C^{cav}$ carbon atoms with hydrogen to methane (b). Submodel 3: cavity growth due to creep and grain boundary diffusion (c).

Submodel 1: Dissolution of carbides

During hydrogen attack, the average carbon composition in the steel decreases which results in a driving force for carbide dissolution, i.e. in a reduction of the Gibbs free energy G of the total system (α-Fe + carbides). Its rate, $\dot{G}$, is linearly related to the size change of the carbides via

$$\dot{G} \equiv \sum_{j=1}^{N} A^j \dot{\rho}^j . \tag{1}$$

The coefficient A^j depends on the actual radius ρ^j of the carbide j, the thermodynamic parameters of the phases α and carbide j, and on their composition. The exact expression of A^j and its derivation can be found in [2]. Here, it is sufficient to mention that all phases are described with the sublattice model [3, 4] where the corresponding thermodynamic parameters have been gathered from the literature (for a complete list see [5]).

During the dissolution of carbide j, $\dot{n}_i^j$ metal and carbon atoms (i = Fe, Cr, Mo and C) transfer across the matrix-carbide interface and diffuse within the ferritic matrix. As the alloy carbides possess a higher content of Cr, Mo and C than the ferritic matrix, these elements diffuse away from the dissolving carbide, while Fe diffuses towards the carbide. For the modelling, it is assumed that the diffusion of the substitutional elements controls the kinetics of the dissolution. Instead of directly solving Fick's second law of diffusion, we express the Gibbs energy dissipation $\dot{Q}_i^j$ associated with the diffusion of component i by [2]

$$\dot{Q}_i^j = \int_V \frac{RTV_m^{Fe}}{y_i^\alpha D_i^\alpha} (J_i^j)^2 dV. \tag{2}$$

with J_i^j the diffusive molar flux, T the temperature, y_i^α the composition of the ferrite, V_m^Fe its molar volume and D_i^α the diffusivity of component i. To bypass the large numerical effort to calculate the fluxes locally, we make the simplification that all k components are and remain homogeneously distributed in the ferritic matrix and that no diffusion takes place inside the carbides. As another simplification, we do not take into account the spatial arrangement of the carbides; instead we imagine that each carbide j sits in the center of our spherical unit cell. Under the assumption that the components remain homogeneously distributed during hydrogen attack, each flux should exhibit the radial dependence $J_i^j(r) = (\dot{n}_i^j/4\pi r^2)(1-r^3/r_\mathrm{o}^3)$, as is illustrated in Figure 1a. This allows us to integrate (2) over the volume of the unit cell. Since there exists a direct relation between $\dot{n}_i^j$ and $\dot{\rho}^j$, the total dissipation $\dot{Q} = \sum_{j=1}^{N}\sum_{i=1}^{k} \dot{Q}_i^j$ can be formulated as a function of the unknown $\dot{\rho}^j$. By inserting (2) and (1) into the condition $\dot{Q} + \dot{G} = 0$ [6] we obtain the size change $\dot{\rho}^j$ of each carbide.

Submodel 2: Chemical reaction

When $\dot{n}_\mathrm{C}^\mathrm{cav}$ carbon atoms in the cavity (located in the center of the unit cell, see Figure 1b) react with hydrogen molecules to form methane, the total Gibbs energy reduces according to

$$\dot{G}_\mathrm{C} = -\dot{n}_\mathrm{C}^\mathrm{cav}\Delta f = \dot{n}_\mathrm{C}^\mathrm{cav}(\mu_{\mathrm{CH_4}} - 2\mu_{\mathrm{H_2}} - \mu_\mathrm{C}^\alpha). \tag{3}$$

Δf represents the driving force and μ_x stands for the chemical potential of the component x. Knowing the actual composition of the ferritic matrix, the actual methane pressure in the cavity and the applied hydrogen pressure, we can calculate this driving force. Besides Δf, the availability of carbon atoms at the cavity-matrix interface plays an important role for the kinetics of the chemical reaction. The more and the faster carbon atoms diffuse in the ferritic matrix towards the cavity, the higher will be the rate of reaction, characterized by $\dot{n}_\mathrm{C}^\mathrm{cav}$. Like in submodel 1, the dissipation energy due to the diffusion of C atoms, $\dot{Q}_\mathrm{C}$, is equal to $-\dot{G}_\mathrm{C}$ which allows us to compute the number $\dot{n}_\mathrm{C}^\mathrm{cav}$ of methane molecules that are newly formed per unit of time.

Submodel 3: Void growth

The gas pressure p_m $(= p_{\mathrm{CH_4}} + p_{\mathrm{H_2}})$ causes the cavity to grow (Figure 1c). Grain boundary diffusion and dislocation creep (described by a Norton law) lead to an increase of the volume of the cavity, $\dot{V}^\mathrm{cav} = \dot{V}_\mathrm{diff}^\mathrm{cav} + \dot{V}_\mathrm{cr}^\mathrm{cav}$. A numerical and analytical analysis of the growth of a representative single cavity was performed by Van der Giessen *et al.* [7] leading to approximate yet accurate closed-form expressions for $\dot{V}_\mathrm{diff}^\mathrm{cav}$ and $\dot{V}_\mathrm{cr}^\mathrm{cav}$. For the sake of brevity we just mention that $\dot{V}_\mathrm{diff}^\mathrm{cav}$ depends linearly on p_m, while $\dot{V}_\mathrm{cr}^\mathrm{cav}$ is proportional to p_m^n with n the creep exponent. The exact expressions are given in [2, 5, 7, 8]. Under the condition that the cavity maintains its equilibrium spherical cap shape during growth, a relation exists between $\dot{V}^\mathrm{cav}$ and the rate of the cavity radius $\dot{a}$.

The outcome of the three submodels are the values for the rates $\dot{\rho}^j$, $\dot{n}_\mathrm{C}^\mathrm{cav}$ and $\dot{a}$. An explicit time integration scheme is applied to obtain the actual ρ^j, $n_\mathrm{C}^\mathrm{cav}$ and a as a function of the exposure time. Based on this information, we update the composition of the ferrite and the methane pressure at each new time instant.

RESULTS

Before we can apply the model, the material parameters (e.g. diffusion coefficients of all components, creep parameters), the operating and the initial conditions should be specified. For the material parameters we refer to [2]. We chose to simulate autoclave tests where 2.25Cr-1Mo steels with different microstructures are exposed to a hydrogen pressure of 18MPa at a temperature of 530°C. The alloy composition is fixed to 2.4at%Cr, 0.58at%Mo and 0.7at%C, while various carbide types and volume fractions are assumed in the calculations. Chao *et al.* [1] found the following carbide types and carbide composition (expressed in site fractions) in their investigation: M_7C_3 with 35%Fe, 60%Cr and 5%Mo; $M_{23}C_6$ with 55%Fe, 39%Cr and 6%Mo; M_6C with 45%Fe, 13%Cr and 42%Mo and M_2C with 3%Fe, 27%Cr and 70%Mo. Unfortunately, the total volume fraction f^carb is not mentioned, just their relative volume fractions: 43% of the total volume occupied by the carbides belongs to M_7C_3, 25% to $M_{23}C_6$, 10% to M_6C and finally 21% to M_2C. As we do not know the value for f^carb, we study two cases. In the first case (microstructure m1), f^carb possesses the maximum possible

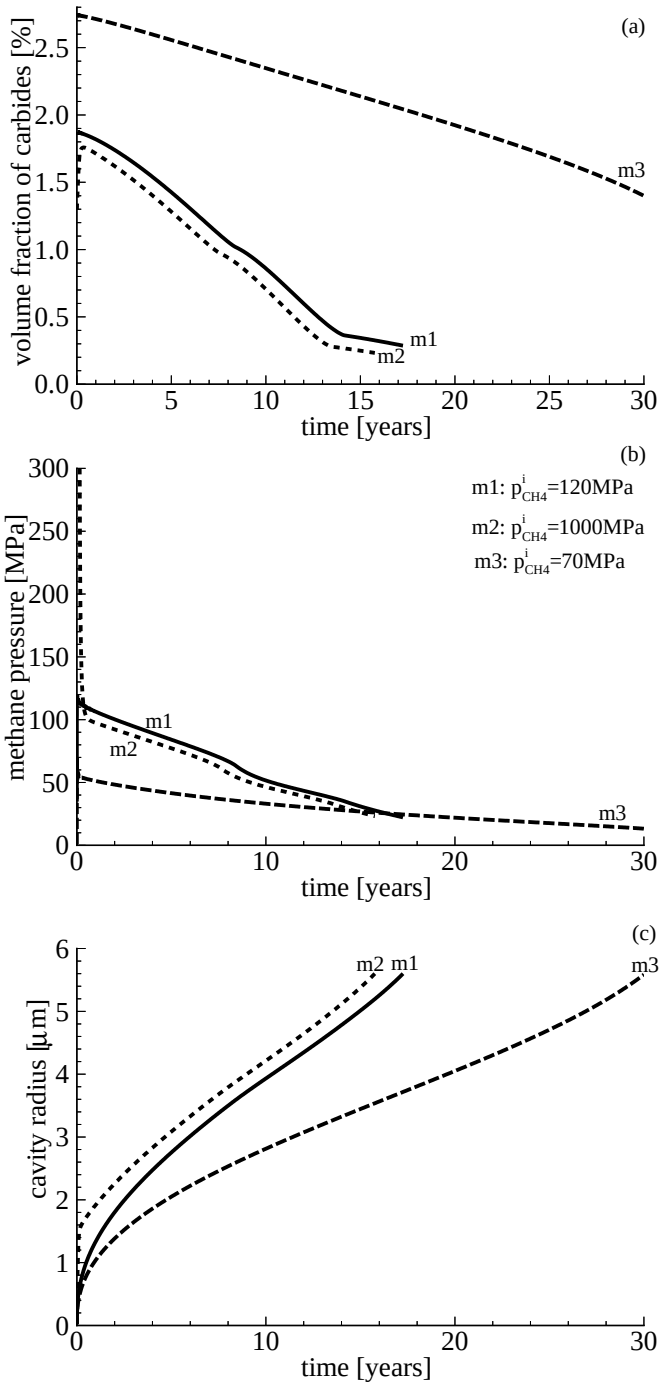

Figure 2: Evolution of the total volume fraction of carbides (a), of the methane pressure (b) and of the void radius (c) for various microstructures (m1, m2, m3) exposed to a hydrogen pressure of 18MPa at a temperature of 530°C.

value, namely $f^{\mathrm{carb}} = 1.87\%$ which then corresponds to the following composition of the ferritic matrix: 1.6%Cr, 0.16%Mo and 2.6×10^{-5}%C. To check the influence of f^{carb} on HA, the second microstructure (m2) contains a smaller carbide volume fraction, $f^{\mathrm{carb}} = 1.3\%$, and a ferritic matrix of 1.9%Cr, 0.29%Mo and 2.2×10^{-1}%C. Further input parameters are the total number of carbides N in the unit cell, their radius ρ^j and the size of the unit cell (r_{o}). For the sake of simplicity, we assume that in a unit cell of the radius $r_{\mathrm{o}} = 8\mu$m there are 100 carbides which all possess the same size. This means that $\rho^j = 0.46\mu$m in m1 and $\rho^j = 0.41\mu$m in m2. According to the measured relative carbide fractions, there are 43 M_7C_3 carbides, 25 $M_{23}C_6$ carbides, 10 M_6C carbides and 21 M_2C carbides in both microstructures. The third microstructure (m3) of interest here is the equilibrium microstructure. We used the thermodynamics program Thermo- Calc [9] to predict the equilibrium state of the 2.25Cr-1Mo steel at a temperature of 530°C in air. The outcome is a microstructure just containing two types of carbides, namely $M_{23}C_6$ (30.8%Fe, 56.5%Cr and 12.7%Mo) with a volume fraction

of $f^{\mathrm{M_{23}C_6}}$ of 2.6% and M_6C (35.6%Fe, 3.1%Cr and 61.3%Mo) with a volume fraction of $f^{\mathrm{M_6C}}$ of 0.16%. Again we assume that there are 100 equally sized carbides embedded in the unit cell. From $f^{\mathrm{M_{23}C_6}}$ and $f^{\mathrm{M_6C}}$ it follows that $\rho^j = 0.52\mu$m and that 94 $M_{23}C_6$ carbides and 6 M_6C carbides are present.

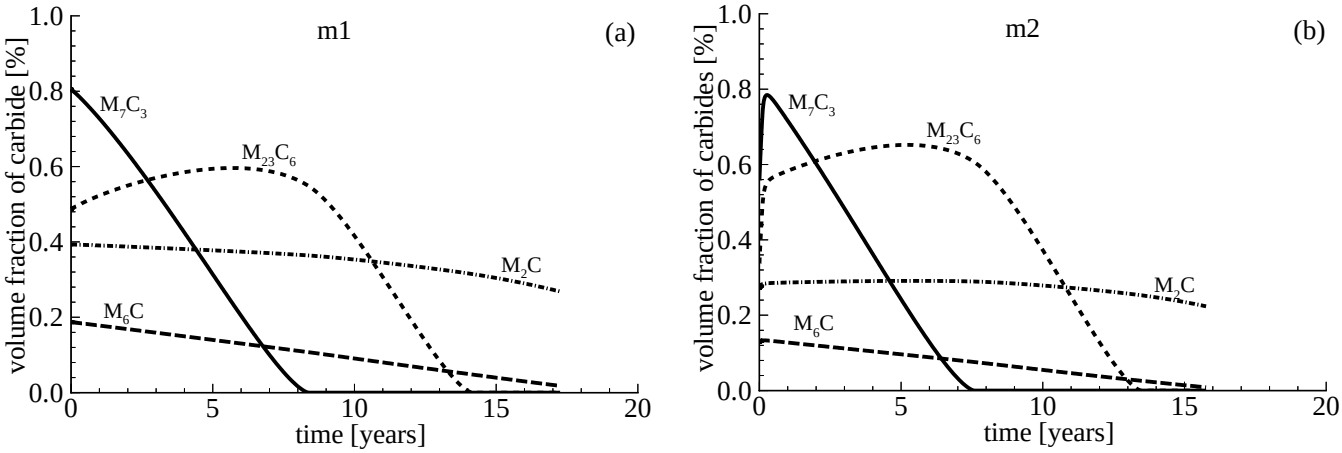

Figure 3: Evolution of the volume fraction of the various carbide types (M_7C_3, $M_{23}C_6$, M_6C, M_2C) during exposure at 530°C in microstructure m1 (a) and microstructure m2 (b).

The model is applied to simulate the response of these three microstructures to hydrogen exposure. Some selected results are shown in Figure 2 giving (a) the volume fraction of all carbides f^{carb}, (b) the methane pressure and (c) the cavity radius as a function of exposure time for each microstructure. Starting with microstructure m1, we see (Figure 2b) that a methane pressure of 120MPa is built up at the beginning of the exposure which leads to void growth (Figure 2c). In order to keep up the methane pressure in a bigger void, new carbon atoms should react with hydrogen to methane. First, the carbon atoms dissolved in the ferritic matrix react. Due to the initially very low carbon content of microstructure m1 (2.55×10^{-5}%C), the reacting carbon atoms mainly stem from the second source, the carbides. As seen in Figure 2a, their total volume fractions decreases. During this dissolution, carbon atoms transfer from the carbide to the matrix where they diffuse to the cavity to react. Carbide dissolution takes time since it is controlled by the diffusion of the substitutional elements Cr and Mo. It is not fast enough to keep the methane pressure at a constant value and indeed it is seen (Figure 2b) to decrease as the cavity grows. In microstructure m2, the ferritic matrix contains a high initial carbon content. As a first consequence, a high methane pressure ($p_{\mathrm{CH_4}} = 1000$MPa) is built up in the cavity and the cavity grows very quickly during the early stages of the exposure. A second consequence is that the carbides grow as long as the carbon content is high and as long as a driving force for precipitation exists. This results in an increase of f^{carb} from 1.3% to 1.9% as seen in Figure 2a. When the carbon content has reached a low value, the methane pressure drops quickly, the void growth slows down and the carbides dissolve similar to microstructure m1. Microstructure m3, which is initially in the equilibrium state, is much less susceptible to HA. The methane pressure (starting with 70MPa and decreasing to 20MPa) is quite low which results in a slow void growth. The carbides also dissolve very slowly.

Now, we have a closer look at the influence of the carbide type on HA. To find out whether they possess a different susceptibility, Figure 3 shows the volume fractions of each carbide type individually, both for microstructure m1 (a) and microstructure m2 (b). In m1, the M_7C_3 carbides dissolve by far the fastest, M_6C and M_2C dissolve much slowlier while the $M_{23}C_6$ carbides seem to be quite stable during the first years. They even grow for the first 6 years (Figure 3a). Except for the early beginning, the picture does not change for microstructure m2. Due to the high initial carbon content in the ferrite, all carbide types grow first and then they behave similar to m1. In microstructure m3 (not shown), the volume fraction of the $M_{23}C_6$ carbides decreases from 2.6% to 1.2% within 30 years while the volume fraction of M_6C remains the same (0.16%). It turns out that the relatively high resistance to HA of m3 is related to the absence of M_7C_3 carbides.

CONCLUSIONS

A microstructural model has been presented which covers the potentially relevant mechanisms responsible for hydrogen attack, such as diffusion of carbon and metal atoms, the chemical reaction to methane, grain boundary diffusion and dislocation creep. The simulation of autoclave tests of 2.25Cr-1Mo steels with different microstructures demonstrates that the methane pressure is not constant during HA, thus falsifying previous decoupled approaches to HA. Then, they show that the methane pressure at the beginning of the exposure is related to the initial carbon content of the ferritic matrix. Microstructure m2 with its high content of dissolved carbon in the ferrite possesses a very high methane pressure initially. Afterwards, the methane pressure drops in all cases, because the cavities grow and the carbides dissolve too slowly to supply sufficient carbon atoms for the reaction. Consequently, the decreasing methane pressure is responsible for a delay in void growth. Furthermore, the simulations reveal the big influence of the carbide types on the failure times. The equilibrium microstructure (m3) which contains just $M_{23}C_6$ and M_6C carbides fails after 30 years. The microstructures m1 and m2, where M_7C_3, $M_{23}C_6$, M_6C and M_2C carbides are present, give rise to failure times of 17 and 16 years. The higher resistance of m3 can be mainly attributed to the absence of M_7C_3, which dissolves quite easily in the other microstructures.

ACKNOWLEDGEMENTS

The work of S.M. Schlögl is supported through the FOM/NIMR research program “Evolution of the microstructure of materials”.

REFERENCES

[1] Chao, B.L., Odette, G.R. and Lucas, G.E. (1988). ONRI/Sub/82-22276/01 University of California, Santa Barbara, United States.

[2] Schlögl, S.M., Svoboda, J. and Van der Giessen, E. (2001), submitted to *Acta Mat.*.

[3] Hillert, M. and Staffansson, L.-I. (1970) *Acta Chem. Scand.* 24, 3618.

[4] Sundman, B. and Ågren, J. (1981) *J. Phys. Chem. Solids* 42, 297.

[5] Schlögl, S.M., van Leeuwen, Y. and Van der Giessen, E. (2000) *Metall. Mat. Trans. A*31, 125.

[6] Svoboda, J. and Turek, I. (1991) *Phil. Mag. B* 64, 749.

[7] Van der Giessen, E., Van der Burg, M.W.D., Needleman, A. and Tvergaard, V. (1995) *J. Mech. Phys. Solids* 43, 123.

[8] Van der Burg, M.W.D., Van der Giessen, E. and Brouwer, R.C. (1996) *Acta Mat.* 44, 505.

[9] Sundman, B., Jansson, B. and Anderson, J.O. (1985) *CALPHAD* 9, 1127.